Experimentation and driving cycle performance of three architectures for waste heat recovery through Rankine cycle and organic Rankine cycle of a passenger car engine.

Olivier Dumont(CA)[a], Rémi Dickes[b], Mouad Diny[c], Vincent Lemort[d]

[a] Thermodynamics laboratory, Liège, Belgium, olivier.dumont@ulg.ac.be
[b] Thermodynamics laboratory, Liège, Belgium, rdickes@ulg.ac.be
[c] PSA GROUPE, La Garenne Colombes, France, mouad.diny@mpsa.com
[d]Thermodynamics laboratory, Liège, Belgium, vincent.lemort@ulg.ac.be

Abstract:

The transportation sector needs to decrease significantly its energy consumption. The Rankine cycle (R) and the organic Rankine cycle (ORC) are two of the most promising technologies to convert waste heat from the internal combustion engine (i.e. from exhaust gas and/or engine cooling system) into mechanical or electrical energy. In this paper, three different system architectures are compared using both experimental and modelling investigations. The first architecture consists in a Rankine cycle (using demineralized water as working fluid) using the exhaust gas waste heat of the engine (R-EG), the second cycle consists in an ORC using the thermal power of the engine cooling system (ORC-CE) and the third consists in an ORC using the exhaust gas waste heat (ORC-EG). The advantages and disadvantages in terms of costs, control, influence of ambient conditions, thermal inertia, weight, additional pumping losses due to the eventual addition of a heat exchanger in the exhaust gas line and part load performance of each architecture is detailed. In terms of fuel saving during a standard driving cycle, this study shows that the ORC-CE is the best architecture (3.5%) followed by the ORC-EG (3.2%) and finally the R-EG (2.7%).

Keywords:

Rankine cycle, organic Rankine cycle, Passenger car, Waste heat recovery, experimental investigation.

1. Introduction

1.1. Context

According to the European directive, cars are responsible for about twelve percent of the total EU emissions of CO2 [1]. Roughly one fourth of the combustion energy is converted into useful work. Generally, the major losses during the combustion are known to be heat losses in the engine coolant and heat losses in the exhaust gas. One solution to reduce the car fuel consumption is to reuse the waste heat released in the exhaust gas and/or in the coolant fluid. Many paper in literature study different architectures for waste heat recovery system based on simulations or experimental results ([2] among others). Most of the papers are related to the long haul trucks due to the stable conditions of the source of waste heat compared to a passenger car [3,4,5]. For the passenger car application, few papers discuss the topic. In 2011, an experimental study [6] demonstrated a 0.5 kW (resp. 0.9 kW) average production on an urban cycle (resp. highway cycle) using the exhaust gas heat source. In 2014, Legros [7] investigated a Rankine power system using the exhaust gas as heat source and a tailor-made scroll expander allowing to decrease up to 6.7 g the emissions of CO2 per km. In 2015 [8], the waste heat from the engine cooling system of a stationary engine was able to increase the

engine power up to 12% through an organic Rankine cycle power system. In 2017 [9], a 1 kW ORC helped to increase the efficiency of an internal combustion engine of 9.3% using both the engine cooling system and the exhaust gas. Also, the combination of both heat sources could be used with hybrid cars showing up to 8.2% consumption decrease [10]. Based on this state of the art, some work remains to be performed. The aim of this paper is to:

- Compare three different architectures of waste heat recovery for a passenger car.
- Evaluate the performance of the components and of the global cycle based on an experimental approach.
- Calibrate models that are able to predict the performance outside the calibration range.
- Simulate the performance in steady-state and on realistic driving cycles for each architecture.
- Compare different architectures and heat sources to identify which is the most promising ones according to different criteria (inertia, part-load performance, maturity, among others).

After this short introduction, section 2 presents the different experimental set-ups and the modelling methodology. Following this, the experimental results and the calibration of the models is performed in section 3. These calibrated models are used to simulate the performance of the different architectures on different driving cycles. In section 4, a comparison between the three architectures to recover the waste heat from the passenger car is performed and discussed. Finally, the conclusion summarizes the main results and introduces promising perspectives.

2. Methodology

2.1. Case study

The case study is a passenger car with a 157 kW gasoline engine (displacement of 1598 cm^3) without exhaust gas recirculation (EGR). The exhaust gas temperature varies between 400°C and 800°C while the engine cooling system temperature can vary between 70°C and 120°C. A manual control allows to regulate finely the accelerator pedal to regulate the shaft speed. This engine is connected to a brake, which is water-cooled. The torque of the brake is also regulated manually. A Coriolis mass flow meter measures the fuel consumption while a lambda probe (i.e. an oxygen sensor) measures the proportion of oxygen in the exhaust gases.

2.2. Experimental set-ups

Three standard configurations are considered in these experimental investigations (Fig. 1):

- A non-recuperative Rankine cycle (demineralized water) using the waste heat available in the exhaust gases (R-EG).

- A recuperative organic Rankine cycle power system (R245fa) using the waste heat available in the cooling water of the engine (ORC-CE).

- A recuperative organic Rankine cycle power system (R245fa) using the waste heat available in the exhaust gases (ORC-EG).

Usually, the simplest way to condense the working fluid is to use the engine cooling system (R-EG). However this would lead to high condensation pressure for the ORC configurations and so to low efficiencies. An air-cooled condenser is therefore preferred for the ORC-EG and ORC-CE configurations.

Three test-rigs are designed and built. Their technical specification is detailed in Table 1.

- **R-EG**: The sizing of the components of the test-rig has been presented in [7]. In this Rankine cycle, two different evaporator have been tested: a counter current (CC) heat exchanger and a hybrid current (HC) heat exchanger. In a first time, a scroll expander, designed for this application [7] is tested. An axial turbine, designed for μCHP has also been investigated [11]. This turbine requires additional components (a steam trap and an inverted bucket separator to

avoid droplets, a second condenser and a void pump to reach the nominal exhaust pressure (≈0.1 bar).

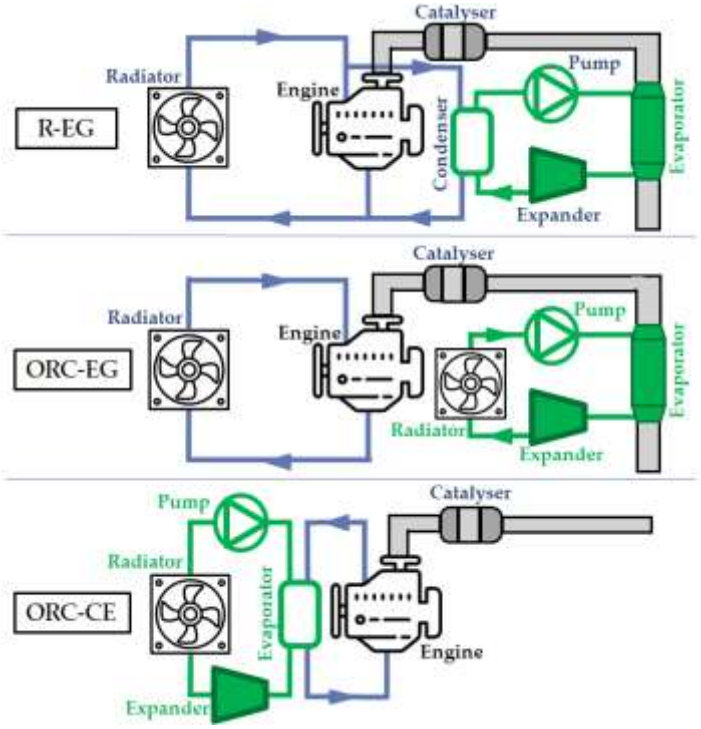

Fig. 1. Schematic representation of the three architectures.

- **ORC-CE:** A 3kWe ORC using R245fa as working fluid is equipped with a recuperator, a brazed plate heat evaporator, an air-cooled condenser and a diaphragm pump. Four types of expanders are tested (Table 1). For more details, please refer to a previous paper [12].
- **ORC-EG:** The same test-rig as for the ORC-CE is used (only the evaporator differs – see Table 1).

For more information about the sensors and the detailed layout of each test-rig, please refer to the appendices (Table A1 and Table A2 and Fig. A1-A3) [14].

2.3. Modelling

All the components are simulated with semi-empirical models. This kind of models relies on a limited number of meaningful equations that describe the most significant phenomena occurring in the process. Such a modelling approach offers a good compromise between calibration efforts, simulation speed, modelling accuracy and extrapolation capabilities [12,13,15]. The different models parameters are tuned to reach a good match between the measurements and the model predictions.

Regarding the heat exchangers, a three-zone moving-boundary model with variable heat transfer coefficients is used. The modelling is decomposed into the different zones of the heat exchanger. Each zone is characterized by a global heat transfer coefficient U_i and a heat transfer surface area A_i. The effective heat transfer occurring in the heat exchanger is calculated such as the total surface area occupied by the different zones corresponds to the geometrical surface area of the component. For more details, see [12].

Volumetric machines are simulated using the grey-box model proposed by [16]. By accounting for the most influent physical phenomena in the expansion process with a limited number of parameters, this model demonstrates a good ability to extrapolate the expander performance out of the calibration

dataset while maintaining low computational times. Also, its general formalism allows to model all types of expanders (screw, piston, scroll and root). More details are available in [16].

Table 1. Technical specifications of the test-rigs.

Component	Characteristics	R-EG		ORC-CE	ORC-EG
Working fluid	Rankine	Water		R245fa	
Evaporator	Type	HC	CC	Plate heat exchanger	Confidential
	Mass [kg]	3.7	6.54	52	Confidential
	Volume [m^3]	2.37	1.96	0.009	Confidential
	Exchange area (wf) [m^2]	0.708	0.254	9.8	Confidential
Expander	Type	Scroll	Turbine	Scroll	Screw, piston and root
	Volume ratio [-]	3	-	2.19	
	Swept volume [cm^3]	8	-	12.74	
	Maximal temperature [°C]	250	220	130	See [13]
	Maximal pressure [bar]	20	10	-	
	Nominal power [kW]	~ 4	1.5	~1	
	Maximal shaft speed [RPM]	15 000	30 000	[1000:8000]	[500:5000]
Pump	Type	Gear		Diaphragm	
	Swept volume [cm^3]	0.5		6.8e-6	
	Maximal mass flow rate [g/s]	20 (5000 RPM)		130	
	Maximal pressure [bar]	20		40	
Condenser	Type	Brazed plate		Air-cooled	
	Number	1	2	3	
	Mass [kg]	1.05	2.2	-	
	Volume [m^3]	1.088	2.05	14	
	Water exchange area [m^2]	0.628	0.88	4.66	

The turbine is modeled following a grey box approach, three conservation equations are used to model the turbine (mass flow rate, momentum and total enthalpy) [11]. The windage, mixing and expansion losses are modeled following a former work [17]. The first calibration parameter is used to model the losses in the divergent (entropic loss coefficient) while the second one is used to model the leakage flow [11].

A semi-empirical model is proposed to predict the mass flow rate and the electrical power consumed by the pump (1,2). Equation (1) evaluates the mass flow rate based on the theoretical mass flow rate minus a leakage loss (*A*) while (2) predicts the power consumption with a constant loss (*B*), a speed proportional loss (*C*) and a term proportional to the internal power (*D*).

$$\dot{m}_{wf,pred} = \rho . N . V_s - A\sqrt{2\rho(P_{ex} - P_{su})} \quad (1)$$

$$\dot{W}_{el,pred} = B + C . N + (1 + D) . \frac{\dot{m}_{wf,pred}(P_{ex} - P_{su})}{\rho} \quad (2)$$

Global model

Once the models for the different components are calibrated, they are connected together in a way to simulate the complete cycle (Fig. 2). Practically, the model is able to simulate the performance the entire system and can be decomposed in:

- Inputs: cold sink supply temperature and glide, hot source temperature and flow.
- Parameters: calibration and geometrical parameters of the pump, evaporator, condenser and expander
- Control variables: the pump speed is adjusted to get the desired superheating and the expander speed is fixed in a way to optimize the net power.
- Outputs: working fluid mass flow rate, thermal power in condenser and evaporator, expander power production, pump consumption…

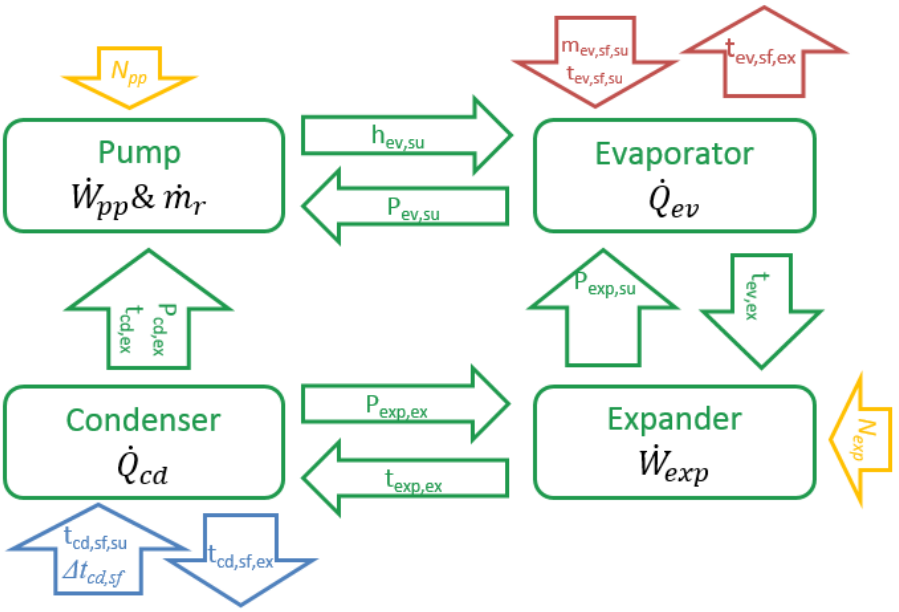

Fig. 2. Modelling of the cycle

2.4. Driving cycle

The most common way to evaluate the consumption and the pollution emissions of vehicles is by means of a driving cycle. The New European Driving Cycle (NEDC) (or Motor Vehicle Emissions Group - MVEG), based on a theoretical driving profile, is used in Europe since 1973. From 2017, the Worldwide harmonized Light vehicle Test Procedure (WLTP) should be preferred since the cycle was developed using real-driving data. In this work, both cycles (NEDC and WLTP) are considered.

A comparison between the NEDC and the WLTP is given in Table 2. As illustrated, the average values of the speed, mechanical power, exhaust gas thermal power, engine cooling thermal power and exhaust gases temperature are significantly lower for the NEDC. The exhaust gas and engine cooling energy are also presented for two situations: (1) when the inertia of the engine is totally neglected (2) in a more realistic cold start situation (heat not available during 800 s for the engine cooling system and 60 s for the exhaust gases). These time constants come from internal confidential data. The ratios of available thermal energy in the exhaust gas over the engine cooling system are equal to 44% and 64% for the NEDC and WLTP respectively. Therefore the NEDC seems more favorable to the CE architecture than the WLTP. Also, the cold start is unfavorable to the engine cooling system because of its high inertia (Table 2).

Table 2. Comparison of the NEDC and WLTP (steady-state, no cold start)

Mean values	NEDC	WLTP
Speed [km/h]	33.8	60.8
Mechanical energy [kWh]	2.75	7.76
Exhaust gas thermal energy [kWh]	1.30	5.02
Exhaust gas thermal energy (cold start) [kWh]	0.91	4.32
Engine cooling thermal energy [kWh]	3.13	6.55
Engine cooling thermal energy (cold start) [kWh]	1.41	4.40
Mean gas temperature [°C]	428	563

The global improvement of the performance of the engine is evaluated using Equation (3) where $\dot{W}_{WHRS}$ is the additional power generated by the considered Waste Heat Recovery System (WHRS), $\dot{W}_{weight}$ is the additional power consumed by the engine because of the additional weight of the WHRS [18] and $\dot{W}_{Ploss}$ is the additional power due to the pumping losses produced in the case of an addition of a heat exchanger in the exhaust gases [19]. In this work, no dynamic is considered. Also, a maximum improvement of performance is evaluated assuming that all the energy produced by the WHRS is useful.

$$\Delta\dot{W}_{WHRS} = \frac{\dot{W}_{WHRS} - \dot{W}_{weight} - \dot{W}_{Ploss}}{\dot{W}_{mec}} \qquad (3)$$

3. Results

3.1. Experimental results

A global methodology including a cross-checking of the measurements, a Gaussian process to delete measurement outliers and a reconciliation method to improve the quality of the data [20] is applied for each experimental campaign. The performance of each component is evaluated in a wide range of conditions. Here is a summary of the main observations:

- **R-EG:** The prototype of pump presents a rather constant volumetric efficiency and an isentropic efficiency (4) reaching 45% (Appendices – Fig. A4), both evaporators presents good performance with efficiencies (6) above 80% (Appendices – Fig. A5) and low pressure drops (Appendices – Fig. A6). However the maximum isentropic efficiencies (5) of the scroll expander (Appendices – Fig. A7) and the turbine (Appendices – Fig. A8) only reach 29% and 42% respectively. The low efficiency of the scroll is explained by high leakages (>50% of the mass flow rate). The turbine cannot be efficient on a real car application since the condensing pressure is very far from the nominal one (0.05 bar). The maximum net production of the cycle is 885 W.
- **ORC-CE:** The performance of the four expanders was compared in [13] and are shown in appendices – Fig. A9. To summarize, the scroll expander shows the highest isentropic efficiency (76%), the screw presents a good adaptability to the working conditions over a wide range of shaft speed ([0-20,000] RPM), the piston expander is well suited for high supply pressure and temperature (up to 250°C and 40 bars) and the root expander is working optimally at low pressure ratios (close to one). In the next part of the work, only the scroll is considered because of its higher efficiency. Working with a more adapted volume ratio (close to 3) and an enlarged port diameter could significantly increase the performance. The evaporator presents a pinch point lower than 5K (Appendices – Fig. A10). The pump reaches

a maximal efficiency (4) of 31% (Appendices – Fig. A11). The maximum net production of the cycle is 754 W. This value could be increased with an optimal sizing (larger piping to decrease pressure drops and optimal design of the expander).

- **ORC-EG:** In the ORC-EG configuration, only the evaporator differs from the ORC-CE layout. This components is rather performing well with an efficiency (6) comprised between 80% and 90% and with pretty low pressure drops on the secondary fluid side (<20 mbars) (Appendices – Fig. A12).

$$\varepsilon_{pp,is} = \frac{\dot{V}_w(P_{ex}-P_{su})}{\dot{W}_{el}} \quad (4)$$

$$\varepsilon_{exp,is} = \frac{\dot{W}_{el}}{\dot{m}_{wf}(h_{su}-h_{ex,is})} \quad (5)$$

$$\varepsilon_{ev} = \frac{\dot{Q}_{ev,sf}}{\dot{m}_{ev,sf,su}.C_{p,eg}(T_{sf,su}-T_{ev,wf,su})} \quad (6)$$

Based on these experimental data, semi-empirical models are calibrated according to section 2.2. The parameters of each model and the accuracy of their prediction is shown in Figures A13-A18 (Appendices) and in Tables A3-A6 (appendices). Models of components are assembled together according to section 3.3 in order to simulate the global performance of the Rankine cycles.

3.2. Simulation results

Using the models developed, it is possible to compare the three architectures in their optimal configuration:

- The R-EG with an optimized theoretical scroll (60% efficiency) and the hybrid current evaporator. This 60% efficiency sounds realistic since leakages can be reduced by adapted coating and adaptation of the axial clearance between the scrolls. The evaporator superheating is fixed to 50K, the sub-cooling is equal to 5K, the shaft speed of the scroll is optimized to maximize the power and the condensation pressure is equal to one.
- The ORC-CE with an optimal theoretical scroll (volume ratio of 3 and supply port diameter increase by a factor 1.5). The evaporator superheating is fixed to 5K, the cooling water exhaust temperature is set to 115°C, the sub-cooling is equal to 5K, the shaft speed of the scroll is optimized to maximize the power and the ambient temperature is set to 15°C.
- R-EG with the optimal theoretical scroll (volume ratio of 3 and supply port diameter increase by a factor 1.5). The evaporator superheating is fixed to 5K, the sub-cooling is equal to 5K, the shaft speed of the scroll is optimized to maximize the power and the ambient temperature is set to 15°C.

Based on these assumptions, the engine power, the WHR performance and the system efficiency of the three architectures are evaluated in function of the vehicle speed (Fig. 3). For each figure featuring the vehicle speed in this paper, the average torque for a given speed on a driving cycle is considered to evaluate the mechanical, exhaust gas and engine cooling powers. The thermal power available in the engine cooling system is higher than the exhaust gas thermal power for speed up to 130 km/h. The efficiency of the R-EG is rather low for low vehicle speeds but reached values comparable to the other cycle for speed higher than 100 km/h. In terms of net Rankine production, the ORC-CE presents the largest value at low speeds but at speeds higher than 120 km/h the R-EG and ORC-EG produce more power. The simulated efficiencies improvement, between 5% and 8.5% are close to the value described in the state of the art (maximum of 9.3% [6,7,9,10]).

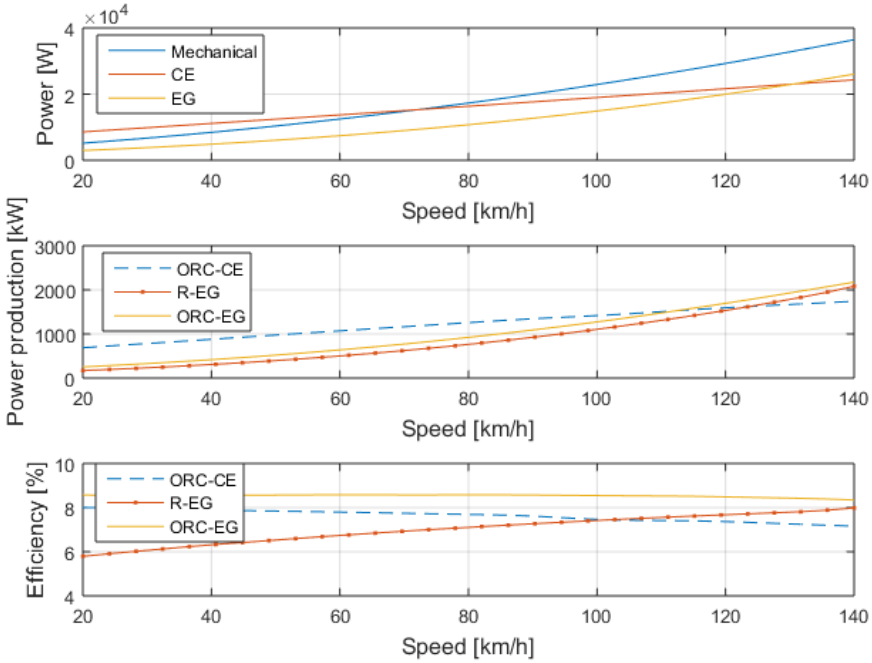

Fig. 3. Engine power, Rankine production and efficiency of the three architectures in function of the vehicle speed. On the top graph, CE and EG represents the thermal power.

Fig. 4 compares the consumption decrease for the three architectures and two driving cycles for "cold start" and "hot start". The cold start takes into account a realistic inertia for the exhaust gases (120 s) and for the engine cooling system (600 s) before starting the Rankine cycle. Practically, the WLTP cycle is probably the most representative of the reality even if no cycle can be considered as perfect. Also, the cold start situation is the most realistic because of the representative inertia taken into account. In the future, car manufacturers plan to use the exhaust gases to heat the engine cooling system at start, which helps at decreasing the cold start time. If this idea is used, the real solution of the system is located somewhere between the "cold start simulation" and the "hot start simulation". The average value of the speed, mechanical power, exhaust gas thermal power, engine cooling thermal power and the exhaust gases temperature are significantly higher for the WLTP (see Table 2). This explains the better performance with the WLTP for the R-EG and ORC-EG architectures that requires high engine loads to perform efficiently.

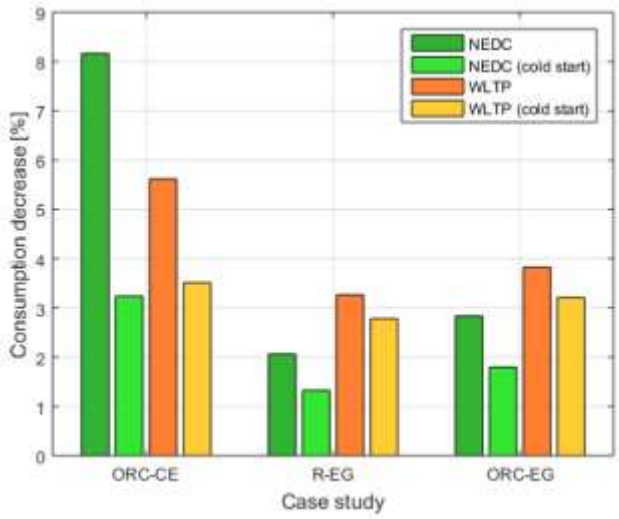

Fig. 4. Improvement of the performance of the engine for three case studies with the NEDC and the WLTP.

4. Discussion

The experimental and simulation results allows to draw some conclusions regarding the advantages and disadvantages of the waste heat source (EG or CE) and of each architecture.

4.1. Exhaust gas (EG) versus engine cooling system (CE)

First a comparison between the advantages and disadvantages of the waste heat source is proposed. The exhaust gas benefits from high temperature (high theoretical Carnot efficiency) and good performance at cold start (low inertia).

Table 3. Comparison between the two WHRS possibilities: EG and CE

Architecture	EG	CE
Energy on a driving cycle	-	+
Part load performance	-	+
Pumping losses produced with the additional heat exchanger in the exhaust gases	-	+
Higher temperature (exergy/efficiency)	+	-
Cold start	+	-

However, the disadvantage of the EG versus the CE are:

- A decrease of the available energy because of the limitation on the exhaust gas temperature to 120°C (condensation issues).
- A large exergy destruction due to expander temperature constraints (max 250°C).
- An additional power consumption due to the pumping losses because of the addition of a heat exchanger in the exhaust gases (Appendices - Figure A6).
- Low part-load energy (Fig. 3).

Table 3 summarizes the comparison between the two WHRS possibilities.

4.2. Comparison between the three architectures

A summary of the different conclusions is proposed in Table 4. Globally, the R-EG and ORC-EG cycle present the maximal performance and a low inertia by valorising the exhaust gas. However, the simplicity, the part-load performance and the relatively low cost (due to the low temperature and large scale production already existing for the HVAC components [21]) of the engine cooling system solution appears promising. On the long term, it is difficult to ensure the chemical stability of the working due to the high gas temperatures. For the ORC-CE, the ambient temperature can have a strong impact on the condensation pressure and, therefore, on the performance. Considering that the WLTP cycle with cold start is probably the most representative of a real situation, the ORC-CE is the best architecture in terms of fuel consumption decrease (3.5%) followed by the ORC-EG (3.2%) and finally the R-EG (2.7%).

Table 4. Comparison of the different architectures

Architecture	R-EG	ORC-EG	ORC-CE
Maximum performance	++	+++	+
Part load performance (driving cycle)	-	-	++
Working fluid stability	++	- - -	++
Influence of ambient conditions	+	+	-
Low investments/maturity/simplicity	-	-	++
Fast start (low inertia)	+	+	-

5. Conclusion

This works aims to compare the performance of different architectures to recover the waste heat in a passenger car. The performance of the components of the cycles are investigated experimentally. Based on these measurements, semi-empirical models are calibrated and used to simulate the performance on different driving cycles.

Based on the experimental and modelling results, an extensive comparison including technology maturity, maximal performance, cold start among others is performed. Based on the most realistic driving cycle (WLTP with a cold start), the ORC-CE presents the highest fuel consumption decrease (3.5%), followed by the ORC-EG (3.1%) and the R-EG (2.85%). Ultimately, the R-EG and ORC-EG systems present the maximal power production at high vehicle speeds (Fig. 3) and a low inertia through the use of exhaust gas. However, the simplicity, the part load performance and the relatively low cost of the engine cooling system looks promising.

Despite the large experimental efforts, this study could be improved by testing other components (axial turbine, piston expander, screw expander) [22] and alternative system architectures [23]. For instance, it could be interesting to combined both sources of waste heat (EG and CE) to benefit from the advantages of each ones (low inertia of exhaust gases and good part load performance of the engine cooling system. Furthermore, the simulations performed here only correspond to one given passenger car (157 kW engine) and the results should be assessed for other cases. For the exhaust gas layouts, the truck applications seems more promising than the car application since it works more often at constant load. Finally, it might be difficult to introduce new fluids in a passenger car due to regulations issues. An elegant way to avoid using a different fluid could be to use the engine cooling fluid as working fluid [24].

Appendices

Available at http://orbi.ulg.ac.be/handle/2268/217510.

Nomenclature

Example:

A calibration parameter,-

B calibration parameter,-

C calibration parameter,-

Cp specific heat at constant pressure, W/(kg m^2)

D calibration parameter,-

h enthalpy, J/(kg K)

$\dot{m}$ *mass flow rate, kg/s*
N *speed [RPM]*
P *pressure, bar*
$\dot{Q}$ *thermal power, W*
t *temperature,* °C
V *volume,* m^3
$\dot{W}$ power, W

Greek symbols

Δ *difference*
ε *efficiency*
ρ *density*

Subscripts and superscripts

el Electrical
ev Evaporator
ex Exhaust
exp Expander
is Isentropic
mec Mechanical
Ploss Pumping losses
pp Pump
pred Predicted
s Swept
sf Secondary fluid
su Supply
wf Working fluid

Acronyms

CE Engine cooling system
EG Exhaust gas
EGR Exhaust gas recovery
NEDC New European Driving Cycle
ORC Organic Rankine cycle
R Rankine cycle
WHR Waste Heat Recovery
WHRS Waste Heat Recovery System
WLTP Worldwide harmonized Light vehicle Test Procedure

References

[1] Union. E., Reducing CO2 emissions from passenger cars. Available: http://ec.europa.eu/clima/policies/transport/vehicles/cars/index_en.htm#top-page (January 2014).

[2] Legros, A., Guillaume, L., Diny, M., Zaïdi, H., Lemort, V., Comparison and impact of waste heat recovery technologies on passenger car fuel consumption on a normalized driving cycle Energies 2014;ISSN 1996-1073.

[3] Guillaume, L., 2017, On the design of waste heat recovery organic Rankine cycle systems for engines of long-haul trucks, PhD thesis, 2017.

[4] Lutz, R., Geskes, P., Pantow, E., Eitel, J., Use of exhaust gas energy in heavy trucks using the Rankine process, MTZ, vol. 73, 2012.

[5] Nelson, C., Exhaust energy recovery, in DEER Conference, 2010.

[6] Hussain, Q., and Birgham, D., Organic Rankine cycle for light duty passenger vehicles, in DEER conference, 2011.

[7] Legros, A., Conception d'un expanseur scroll adapté à la récupération d'énergie à l'échappement pour une application automobile : Aspects thermodynamiques et tribologiques, PhD thesis 2014, Liege, Belgium.

[8] Fu, J., Liu, J., Xu, Z., Deng, B., Liu, Q.,.An approach for IC engine coolant energy recovery based on low-temperature organic Rankine cycle, Journal of Central South University February 2015, Volume 22, Issue 2, pp 727–734 |

[9] Lu, Y., Roskilly, A., Jiang, L., Chen, L., YU, X., Analysis of a 1 kW organic Rankine cycle using a scroll expander for engine coolant and exhaust heat recovery, Energy 2017, 11(4): 527–534

[10] Boretti, A., Recovery of exhaust and coolant heat with R245fa organic Rankine cycles in a hybrid passenger car with a naturally aspirated gasoline engine, Applied Thermal Engineering, Volume 36, April 2012, Pages 73-77

[11] Dumont, O., Diny, M., Lemort, V., Experimentation and modelling of a 1.5 kW axial turbine for waste heat recovery on a passenger car through the use of a RANKINE cycle, 4th EORCC Workshop, Detroit 2017.

[12] Dickes, R., Dumont, O., Daccord, R., Quoilin, S., Lemort, V., Modelling of organic Rankine cycle power systems in off-design conditions: An experimentally-validated comparative study, Energy 2016, 10.1016/j.energy.2017.01.130.

[13] Dumont, O., Dickes, R., Lemort, V., Experimental investigation of four volumetric expanders, Energy Procedia 2017, Volume 129, Pages 859-866.

[14] Dumont, O., Online appendices of the paper "Experimentation and driving cycle performance of three architectures for waste heat recovery trough Rankine cycle and organic Rankine cycle of a passenger car engine". Available at http://orbi.ulg.ac.be/handle/2268/217510.

[15] Dumont, O., Dickes, R., Lemort, V., Extrapolability and limitations of a semi-empirical model for the simulation of volumetric expanders, Energy Procedia 2017, Volume 129, Pages 315-322.

[16] Lemort, V., Declaye, S, Quoilin, S., Experimental characterization of a hermetic scroll expander for use in a micro-scale Rankine cycle, P. I. Mech. Eng. A-J., Pow. 2012, 226, 126-136.

[17] Horlock, J. H., Axial flow turbines: fluid mechanics and thermodynamics, Krieger Publishing Company, 1973.

[18] Koffler, C., Rohde-Brandenburger, K., On the calculation of fuel savings through lightweight design in automotive life cycle assessments, International Journal of Life Cycle Assessment 2010, 15.1, pp. 128– 135. ISSN: 09483349. DOI: 10.1007/s11367-009-0127-z (cit. on p. 192).

[19] Pascual, L., Study of Organic Rankine Cycles for Waste Heat Recovery in Transportation Vehicles, PhD thesis, 2017, Valencia.

[20] Dumont, O., Quoilin, S., Lemort, V., Importance of the reconciliation method to handle experimental data in refrigeration and power cycle: application to a reversible heat pump/organic Rankine cycle unit integrated in a positive energy building, International Journal of Energy and Environmental Engineering 2016, 7(2).

[21] Dumont, O., Quoilin, S., Lemort, V., Experimental investigation of a scroll unit used as a compressor and as an expander in a reversible Heat Pump/ORC unit, Conference: 2014 Purdue Conferences: Herrick Conferences.

[22] Dumont, O., Dickes, R., Lemort, V., Experimental investigation of four volumetric expanders, Energy Procedia 2017, Volume 129, Pages 856-866.

[23] Zhoua, F., Joshia, S., Rhote-Vaney, R., Dedea, E., A review and future application of Rankine Cycle to passenger vehicles for waste heat recovery, Renewable and Sustainable Energy Reviews 2017 75, 1008–1021

[24] Ziviani, D., Donghun, K., Subramanian, S., Braun, J., Groll, E., Feasibility Study of ICE Bottoming ORC with Water/EG Mixture as Working Fluid International Seminar on ORC Power Systems 2017, ORC2017 13-15 September 2017, Milano, Italy